JOURNAL OF AIRCRAFT
Vol. 29, No. 6, Nov.–Dec. 1992

# Unsteady Wind-Tunnel Interference in Aircraft Dynamic Experiments

Martin E. Beyers*
*Institute for Aerospace Research, Ottawa, Ontario, Canada*

**An analysis of existing oscillatory and rotary test data was undertaken to identify the origins of the observed wind-tunnel interference effects and interpret the aircraft aerodynamic characteristics. Logical arguments based on the limited experimental data point to the existence of interference flow mechanisms involving the coupling between unsteady flowfields near the model, the tunnel walls, and around the model support. Oscillatory cross-coupling derivatives measured on the standard dynamics model were significantly affected at low angles of attack while the nonlinear yawing moment characteristics of the HIRM 2 aircraft configuration at high incidence were masked completely in rotary tests performed in a small test section. Both of these very different problems may be attributed to unsteady wind-tunnel interference. Analytical corrections are not feasible at present, but experimental solutions can be implemented. Predictions of vehicle dynamics at high alpha based on dynamic wind-tunnel data can be affected by the interpretation given to the prevailing interference flow phenomena.**

## Nomenclature

$b$ = wingspan
$b_s$ = span of rotor arm
$c$ = $\bar{c}/b$
$C$ = aerodynamic coefficient; with no superscript, in body axes system
$C_{ij}$ = $\partial C_i/\partial(jd/2V)$, $i = \ell, m, n$; $j = q, q', \dot{\alpha}, \dot{\sigma}$ $(d = \bar{c})$; $j = p, \dot{\beta}(d = b)$
$C_{ik}$ = $\partial C_i/\partial k$, $i = \ell, m, n$; $k = \alpha, \beta, \sigma$
$C_\ell$ = rolling moment coefficient, $L/(q_\infty Sb)$
$C_m$ = pitching moment coefficient, $M/(q_\infty S\bar{c})$
$C_n$ = yawing moment coefficient, $N/(q_\infty Sb)$
$C_{yf}$ = fin side-force coefficient
$\bar{c}$ = mean aerodynamic chord
$L, M, N$ = rolling, pitching, and yawing moments
$p_s$ = local static pressure
$p_t$ = wall static pressure
$p_0$ = stagnation pressure
$M_c$ = corrected Mach number
$M_\infty$ = freestream Mach number
$p, q, r$ = body-axes angular velocities
$q'$ = aerodynamic-axes pitch rate
$q_\infty$ = freestream dynamic pressure
$Re$ = Reynolds number based on $\bar{c}$
$S$ = reference area
$V$ = freestream velocity
$w$ = minimum dimension of test section
$x_t$ = longitudinal tunnel coordinate
$\alpha, \beta$ = angles of attack and sideslip
$\Delta$ = increment or amplitude
$\sigma$ = total angle of attack; $\sigma = \cos^{-1}(\cos\beta\cos\alpha)$
$\phi$ = roll angle
$\hat{\phi}$ = bank angle; $\hat{\phi} = \tan^{-1}(\tan\beta/\sin\alpha)$
$\phi'$ = roll orientation angle; $\phi' = \hat{\phi} + n\pi$, $n = 0, 1$
$\Omega$ = coning rate; parameter $\Omega b/2V$
$\bar{\omega}$ = reduced circular frequency, $\omega d/(2V)$, where $d = \bar{c}$ or $b$, as appropriate

*Superscripts*
$\dot{}$ = differentiation with respect to time
$\hat{}$ = aerodynamic axes system
$\bar{}$ = composite fixed-axis derivative
$\tilde{}$ = oscillatory condition

## Introduction

IN rotary balance[1–4] as well as oscillatory test techniques,[1,5–7] the test apparatuses and support systems are necessarily massive to provide the required structural stiffness and force the desired model motions. The sources of support interference[8–11] and unsteady wall interference[12–14] at high $\alpha$ have been identified and analyzed. In contrast to the practice in static balance testing (where extensive calibrations are commonly used to account for the effects of support interference on the aerodynamic characteristics), in high-$\alpha$ dynamic tests these effects cannot simply be "calibrated out." The prerequisite for the implementation of appropriate analytical[8] and experimental[13,15] correction methods is a thorough understanding of the physical flow phenomena involved.

Under conditions encountered in high-$\alpha$ dynamic tests in high-speed wind tunnels, the difficulties are further compounded due to the coupling between the unsteady support and wall interference mechanisms. When this synergism exists, the conventional aerodynamic testing wisdom is not likely to account for the significant effects on the measurements that can be expected.

This article addresses this question, examining the nature of the coupled interference phenomenon referred to here as "unsteady wind-tunnel interference," and identifying the conditions under which it could occur. The hypothesis is supported by experimental results from both rotary and oscillatory tests performed on the HIRM 2 combat aircraft configuration[4] and the standard dynamics model (SDM),[5–7] respectively.

## Background

The primary sources of aerodynamic support interference are those occurring at 1) low $\alpha$, in which the normal development of the wake is terminated by the presence of the support and the disturbance is characterized by a convective time lag[8]; and 2) at high $\alpha$, when vortices generated by a forebody and/or swept-wing surfaces or leading-edge extensions (LEX) interact with a downstream obstacle causing or affecting the vortex burst.[10,11]

The main sources of unsteady wall interference include vortex-wake/wall interference[13] at high $\alpha$, the fluctuating pressure

Presented as Paper 91-0682 at the AIAA 29th Aerospace Sciences Meeting, Reno, NV, Jan. 7–10, 1991; received May 9, 1991; revision received Feb. 12, 1992; accepted for publication Feb. 13, 1992. 

*Senior Research Officer. Member AIAA.

gradients due to unsteady separation in the diffuser or on the walls downstream of the support and to the motion of the model and/or rig,[13] and transverse acoustic interference.[12] If the tests are restricted to nonresonant frequencies, as is usually the intention, the latter can be dispensed with in this discussion.[14] The fluctuations in the pressure gradients caused by model or support motion are superimposed on the static pressure gradients due to the presence of the support[9] and to the test-section flow characteristics.[7] In particular, the flow near ventilated walls is inherently inhomogenous and will contribute to the unsteadiness in dynamic tests.

Unsteady wind-tunnel interference arises when the disturbances generated at the walls (due, for instance, to vortex-wake/wall interaction) and/or in the regions between the support and wall are communicated upstream to the model by way of the flowfield around the support. In the case of a rotary test, the perturbations cause the intrinsically steady support interference to give way to an unsteady type of interference.[13,14] When such conditions prevail, pure support interference, per se, cannot exist.

The effects of tunnel turbulence would tend to modify this motion-induced unsteadiness, although this is not expected to be a major factor here.

## Oscillatory Experiment

Pitch oscillation tests of the SDM[6] were conducted at Mach 0.6 in the IAR 0.75 × 0.40 m dynamics wind tunnel (DWT), which has a rather unusual, asymmetrical test section with one slotted wall. The wingspan to test-section width ratio was $b/w = 0.6$. A side support system[6,9] mounted on the reflection-plane wall of the test section was used (see Fig. 1). The model was set at a mean angle of attack of 10 deg and sideslip angles of ±5 deg, and oscillated in the plane of the total angle of attack. The degree of asymmetry in the measured cross and cross-coupling derivatives was investigated by varying the angle between the symmetry planes of the model and tunnel while maintaining a fixed attitude $\alpha = 10$ deg and $|\beta| = 5$ deg.

Figures 2 and 3 show the cyclical dependence of the cross-coupling derivatives on the roll orientation angle $\phi'$. The overall dynamic interference is clearly significant; the variations in the dynamic derivatives with $\phi'$ were of the order of magnitude of that produced by a 5 deg sideslip increment.[9] The direct opposition between the interference effects on the static and dynamic rolling moment derivatives (Fig. 3) is indicative of the presence of a convective time lag similar to that found for support interference on bodies of revolution[8]; however, this behavior is not apparent in the yawing moment derivatives (Fig. 2). In order to elucidate this phenomenon, the possible origins of wind-tunnel interference are analyzed.

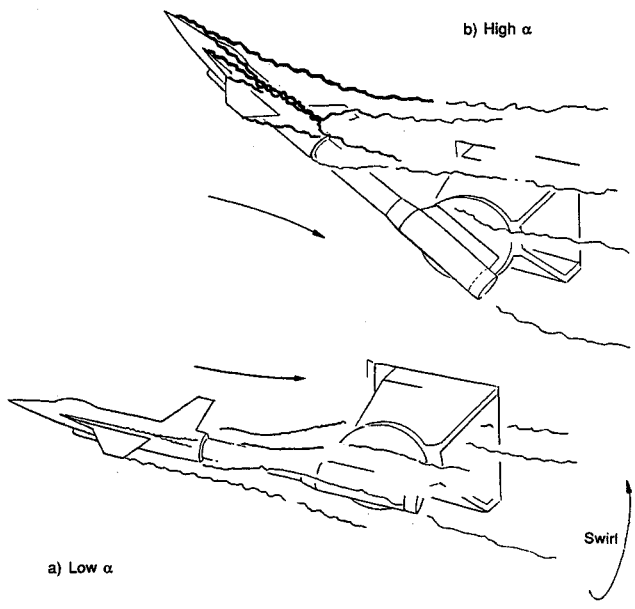


Fig. 1 Aircraft model on sidewall support system.

### Effects of Flow Nonuniformity

The slotted wall in the DWT test section provides sufficient ventilation to eliminate solid blockage caused by 2.5% blockage, streamlined models at transonic Mach numbers.[16] On the other hand, the presence of a similarly sized object producing extensive separation regions will induce significant mass flow through the plenum chamber, resulting in adverse upstream pressure gradients and downstream wake blockage effects as can be seen in Fig. 4. The wall static pressure signatures depicted in Fig. 4 were measured with the SDM on its side support at various angles of attack. While the local influence of the support base is appreciable downstream of the test-section centerline ($x_t > 0$), it is the relative displacement of

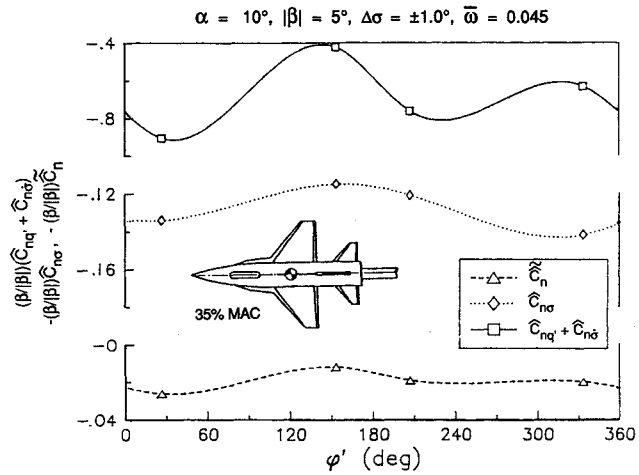


Fig. 2 Effect of sting roll orientation on SDM yawing moment derivatives.

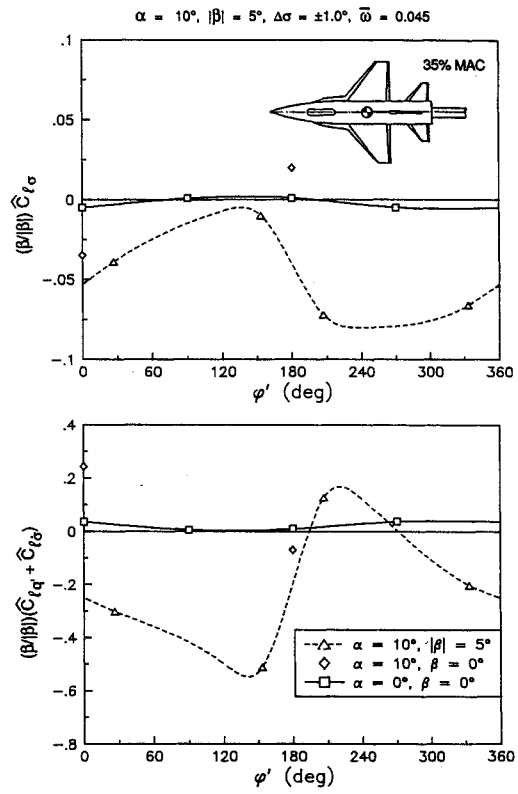


Fig. 3 Effect of sting roll orientation on SDM rolling moment derivatives.

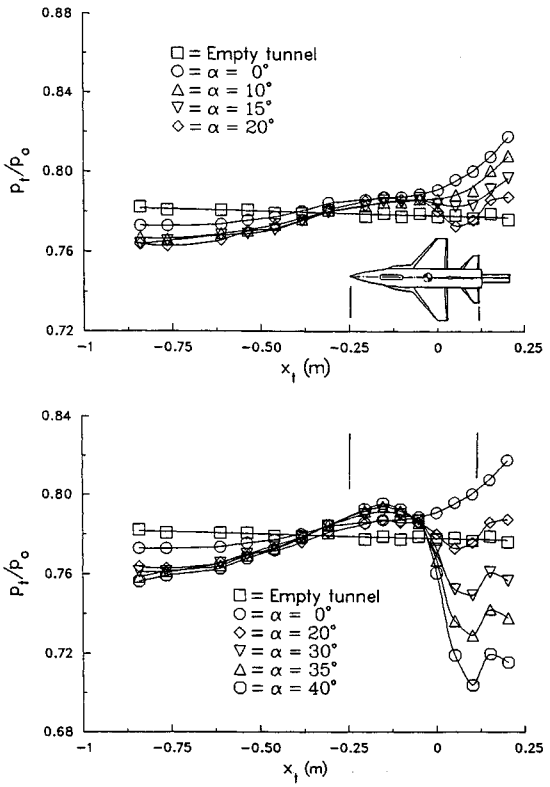


**Fig. 4 Wall static pressure signatures.**

the curves that is of interest. From these results it is clear that flow asymmetries caused by the plenum flow, as well as those due to the presence of the model and support, extend across the entire test section. Therefore, both lateral and longitudinal pressure gradients are present.

Since the outer boundaries are asymmetrical for the centrally mounted SDM, the flow is inherently inhomogeneous. Moreover, the model wake is distorted asymmetrically as it negotiates the pitch platform mechanism at the base of the sting at low to medium $\alpha$ (see Fig. 1a). The disturbed region extends forward of the sting flare, probably well within the critical length for upstream interference[9] $\ell_s/d \approx 2$–2.5. Therefore, it is likely that the present sting length $\ell_s/d = 3.1$ was not sufficient to avoid support interference.

For an oscillating model, the wake blockage and, therefore, the bypass flow through the plenum fluctuates synchronously with the variation in total angle of attack. Figure 4 shows that the flow fluctuations in the test section can be significant because, for the angle-of-attack excursion in these tests $2|\Delta\sigma| \approx 2$ deg, the static effects on the pressure gradients near the solid wall are appreciable along the model length. In the dynamic case the pressure fluctuations at the wall will lag the motion of the model by a characteristic phase angle.

The wall pressure gradients are appreciable at all angles of attack by virtue of the significant strut blockage, but become particularly large once the wing has begun to stall, at $\alpha > 15$ deg. However, while the support produces sufficient wake blockage to induce the upstream pressure gradients, it is the model motion at incidences high enough to produce flow separation that generates the unsteady effect. At $\alpha \to 0$ the wake blockage of the model is near zero and the unsteady effect is absent.

#### Unsteady Wind-Tunnel Interference at Medium $\alpha$

From the above discussion it follows that for the SDM oscillating at low to medium angles of attack ($\alpha \leq 15$ deg) convective communication is present with both the support and walls. The model wake is entrained on the support as in Fig. 1a, resulting in a continuous separated region extending downstream of the support. By altering the flow through the

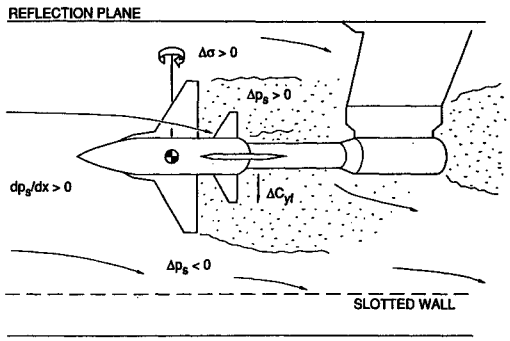


**Fig. 5 Flow response to pitch change at medium $\alpha$.**

plenum, the flow throughout the entire test section is subjected to disturbances (see Fig. 5). The concomitant perturbation of flow around the support will be communicated upstream to the model, but with a time lag different from that associated with direct communication between the model and sting support. Similarly, the direct communication between the model and the side-walls would introduce yet another time lag. Thus, there are at least two convective time lags present.

This interpretation is consistent with the results in Fig. 2; the absence of direct opposition between the effects on $\hat{C}_{nq'} + \hat{C}_{n\dot{\sigma}}$ and $\hat{C}_{n\sigma}$ is indicative of the presence of more than one convective time lag. Interference effects associated with the individual time lags are not simply superimposed but are aspects of a single complex phenomenon involving the coupling between these effects. On the other hand, the opposition between the interference effects on $\hat{C}_{\ell q'} + \hat{C}_{\ell\dot{\sigma}}$ and $\hat{C}_{\ell\sigma}$ in Fig. 3 indicates that in this case the interference is associated with a single dominant convective time lag.

Consider the nature of the flowfield interactions giving rise to dynamic reactions on the aircraft model. The flow response to a positive pitch change $\Delta\sigma$ at low-to-medium angles of attack is conceptualized in Fig. 5. Upstream of the model, the test section flow is essentially two-dimensional. Thus, a change in the plenum flow rate will result in a change in flow curvature in the horizontal plane. With the model at $\alpha = 10$ deg and roll angles of $\pm 26.7$ deg in these tests, the main result of a change in the horizontal flow curvature would be an increment in the side force $\Delta C_{yf}$ exerted on the vertical fin. A pitch increment $\Delta\sigma$ would result in a dynamic yawing moment increment $\Delta C_{n\dot{\sigma}}$ dependent on $\phi'$, but the effect on the rolling moment would be small. The associated time lag would be determined by the time $\Delta t$ required for communication between the model and the slotted wall. Downstream of the model a three-dimensional swirling motion develops as the flow passes over the support (see Fig. 1a). Therefore, disturbances convected upstream from the support are inherently nonplanar, acting on the model lift surfaces to induce a dynamic rolling moment $\Delta C_{\ell\dot{\sigma}}$.

Deflection of the LEX vortex system could also result in dynamic reactions on the aircraft model. Although too weak at $\alpha = 10$ deg to influence the normal force appreciably, the LEX vortices are likely to have some effect on the dynamic reactions as they pass close to the wing at this attitude. This can be seen in the SDM data obtained at AEDC,[17] shown in Fig. 6. The removal of one strake[17] produces a cross-coupling moment derivative $C_{\ell q} + C_{\ell\dot{\alpha}}$ much larger at $\alpha = 10$ deg and $\beta = 0$ deg than that for the symmetrical aircraft at $\beta = 5$ deg. The effects of differential deflections of the LEX vortex system on $\hat{C}_{\ell q'} + \hat{C}_{\ell\dot{\sigma}}$ for the complete aircraft at $\beta = 5$ deg may, therefore, reasonably be expected to be substantial.

The question is, which of the sources of interference identified provide the dominant contributions to the interference present in these results. In the case of the rolling-moment derivatives, the interference has to derive from a nonplanar flow mechanism; this is likely to be the low-$\alpha$ coupled interference occurring through communication by way of the slotted wall and the support. As indicated above, the unsteady

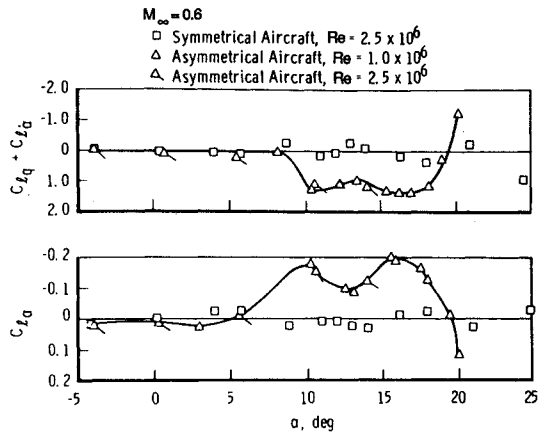


**Fig. 6 Effect of removing left-hand strake on SDM derivatives (Ref. 17).**

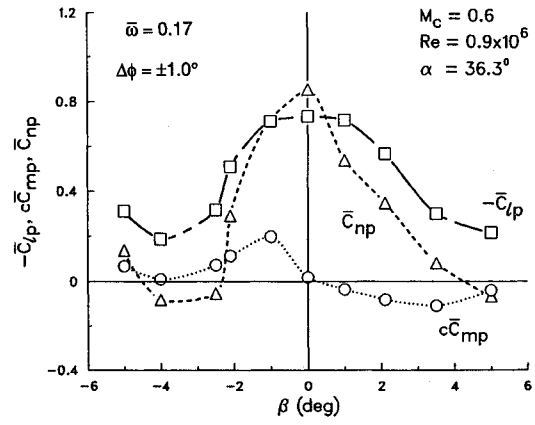


**Fig. 7 Effect of $\beta$ on SDM dynamic derivatives at high $\alpha$.**

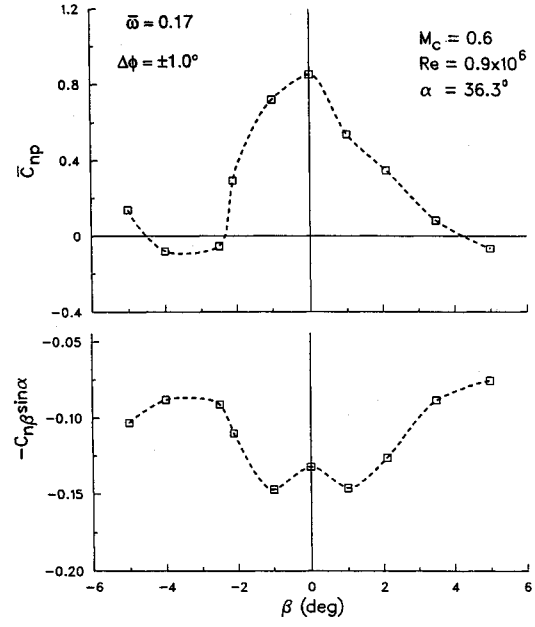


**Fig. 8 Effect of $\beta$ on SDM yawing-moment derivatives.**

wall interference effect on $\hat{C}_{\ell_{q'}} + \hat{C}_{\ell_{\dot\alpha}}$ is small, while the well-known low-$\alpha$ support interference is not a factor as can be seen from the results at $\alpha = \beta = 0$, which exhibit negligible interference (see Fig. 3). Since one convective time lag clearly dominates, the contribution of unsteady wall interference effects on the LEX vortex system is thought to be less important.

In the yawing moment data the communication by way of the slotted wall and support is again considered significant but, in this case, this flow mechanism is coupled with the unsteady wall interference due to communication between the model and the slotted wall. Interference effects on the LEX vortices are negligible here since the strakes do not appreciably affect the yawing moment derivatives[17] at $\alpha = 10$ deg. Direct communication between the model and support may have been present in addition, but it is likely that the wall effects were dominant. Therefore, there are two convective time lags present, accounting for the form of the $\phi'$ dependence in Fig. 2.

In this interpretation the different effects on the rolling and yawing moment derivatives are manifestations of a complex, unsteady wind-tunnel interference mechanism. A single convective time lag associated with the coupled support/wall interference is dominant in the former case, whereas additional coupling is produced by the unsteady wall interference, introducing a second time lag that mainly influences the yawing moment derivatives. In general, the nature of the interference is determined by the configuration type and installation geometry. In other tests, such as those involving a low fineness-ratio body, the direct communication between the model and support[8] may be important in addition to other effects present.

#### Unsteady Wall Interference at High $\alpha$

At high angles of attack the scenario is simplified considerably since the vortex wake effectively passes above the support as illustrated conceptually in Fig. 1b. Therefore, the coupled wall/support interference occurring at angles of attack of about 15 deg and lower is absent. Vortex-wake/wall interference[13] is likely to occur as the forebody and strake vortices are perturbed by the effects of disturbances at the walls on vortex burst and core trajectory. However, a form of coupled interference may yet be present during pitch oscillation because of the presence of disturbances originating at the slotted wall. This will be similar to the flow mechanism described above with reference to Fig. 5, except that the separation region of interest is now confined to the model wake and the flow fluctuations will act on the vortex system. Thus, in general, there are two unsteady wall interference mechanisms present, resulting in two convective time lags.

There is some evidence of unsteady wall interference in the SDM roll oscillation tests[5] at $\alpha = 36$ deg and a series of sideslip angles ($-6$ deg $\leq \beta \leq 6$ deg). The lateral-directional aerodynamic coefficients were essentially free of distortion, displaying the expected asymmetrical trends. Thus, the lack of symmetry in the dynamic derivatives[7] with respect to $\beta = 0$ deg apparent in Fig. 7 may be attributed to unsteady wall interference. Since the pitch-angle change corresponding to a roll increment $|\Delta\phi| = 2$ deg is only $\Delta\sigma = 0.05$ deg, the plenum flow perturbation is small so that vortex-wake/wall interference can be expected to be dominant in this case. This is in agreement with the results in Fig. 8, which show that the interference effects on the static and dynamic derivatives are in opposition.[7]

The exact nature of the flowfield interactions producing the dynamic reactions remains to be studied, but it seems likely that the nonlinear pressure gradients in the vicinity of the forebody/LEX vortex system would tend to delay the LEX vortex burst during one part of the oscillation cycle and promote it during the other. A conclusive analysis of the phenomenon would require comprehensive flowfield data from flow visualization or other techniques.

## Rotary Balance Experiment

The second example of unsteady interference discussed here involves rotary data on the HIRM 2 combat aircraft configuration at high $\alpha$ obtained by O'Leary[4] at the Royal Aeronautical Establishment (RAE) in England. Tests were conducted with the model on the same rotary balance apparatus in two different, rather large wind tunnels: 1) the 4 × 2.7 m

low-speed wind tunnel (LSWT) at RAE Bedford; and 2) the 2.4 × 1.8 m variable-density transonic wind tunnel (TWT) at RAE Farnborough. Figure 9 shows the geometrical layout in the 4 × 2.7 m atmospheric tunnel, with the model on a sting-strut at $\alpha = 60$ deg. The relative dimensions in the LSWT and TWT were $b_s/w = 0.4$ and 0.6, respectively.

**Support and Wall Interference**

The effects of downstream interaction between forebody vortices and a support strut or arm can be large, especially when the vortex system becomes asymmetrical at high $\alpha$.[10,11] The interference is basically steady in lunar coning motion. Because of the coning-induced tilting of the forebody vortices, the active vortex could miss the rotor arm at certain angle-of-attack and sideslip combinations when the rotation rate is high enough,[11] thereby alleviating the interference. However, some interference may still be present owing to the distortion of the flowfield by the rotor arm.

In a rotary test, vortices generated by the forebody and lift surfaces are convected downstream as coaxial helical structures of common pitch, sweeping around in a circular path. The close proximity of wind-tunnel boundaries could distort these vortex formations cyclically. This has been referred to as vortex-wake/wall interference.[13,14] When the span of the rotor arm is large $b_s > b$, as is usually the case at high $\alpha$, the trailing tip vortices will be the prime source of vortex-wake/wall interference. As the vortex trails move towards or away from a point on the wall, boundary-layer separation could occur on the wall or further downstream, in the diffuser, as illustrated in Fig. 10. Thus, the separation line on the wall/diffuser would oscillate longitudinally while traveling in the direction of the rotation. Concomitantly, the wake blockage and upstream pressure gradients would fluctuate with the associated velocity-deficient region.

In a solid-walled test section the disturbances originating from the separation regions on the walls would interact with the flowfield around the rotor arm, thereby distorting the model wake. In a ventilated test section (such as in the TWT) periodic disturbances generated by the passage of the wake near the wall would extend into the test section in much the same way as that demonstrated in the oscillatory experiment (see Fig. 4), producing similar distortions of the wake flow. Hence, the flowfield disturbances associated with model/support and support/rotor/wall interactions are coupled, and the interference on the model becomes unsteady.

The presence of fixed support structures, such as the vertical tunnel fairing downstream of the rig in the TWT,[18] would tend to produce an unsteady effect on the rotating model through periodic interruption of the wake, but since these disturbances are of relatively short duration and the support struts are quite far downstream, it is felt that the associated effects on the time-averaged $C_n$ measurements would have been small.

*HIRM 2 Rotary Test Data*

A comparison of results from the rotary balance tests of HIRM 2 at $\alpha = 60$ deg revealed dramatic discrepancies between the body-axes yawing moments measured in the two wind tunnels[2,4] at the same Reynolds number $Re = 1.35 \times 10^6$ (see Fig. 11). The unstable characteristics at small $\Omega b/2V$ observed in the LSWT are not present in the measurements from the smaller facility. When the test in the LSWT was repeated subsequently[18] the bistable behavior was again absent (Fig. 12), suggesting a high degree of sensitivity to test conditions. Tests at a higher Reynolds number $Re = 3.81 \times 10^6$ in the pressurized tunnel showed a reduced slope of the yawing moment characteristic, particularly at medium $\Omega b/2V$ values, but again failed to reproduce the unstable trend at low rates. Moreover, the trend of decreasing stability with increasing $Re$ was not observed in the low $Re$ data (Fig. 12). At a lower angle of attack $\alpha = 20$ deg, there was little effect due to either Reynolds number[4] or size of test section.[2]

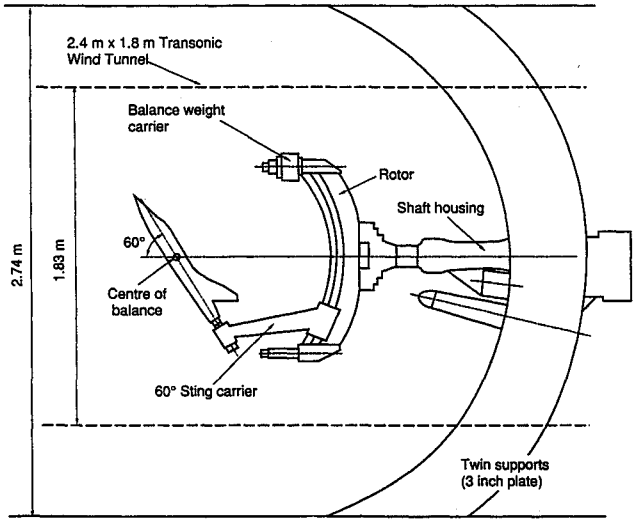


**Fig. 9 Layout of RAE rotary balance in 4 × 2.7 m low-speed wind tunnel.**

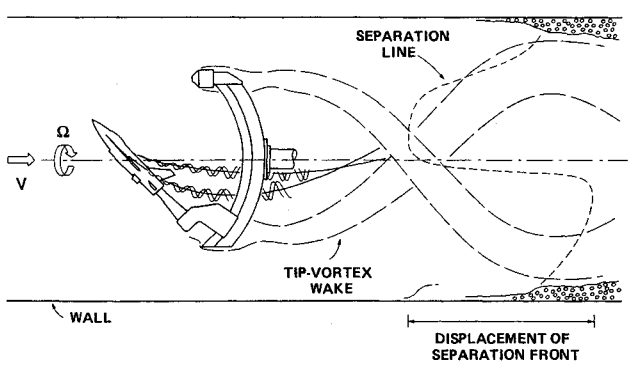


**Fig. 10 Coupled support/wall interference in rotary test.**

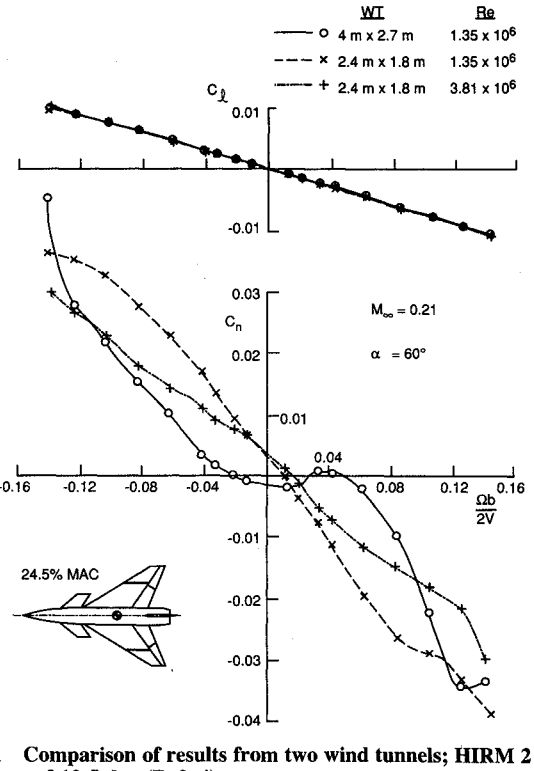


**Fig. 11 Comparison of results from two wind tunnels; HIRM 2 with LE droop of 12.5 deg (Ref. 4).**

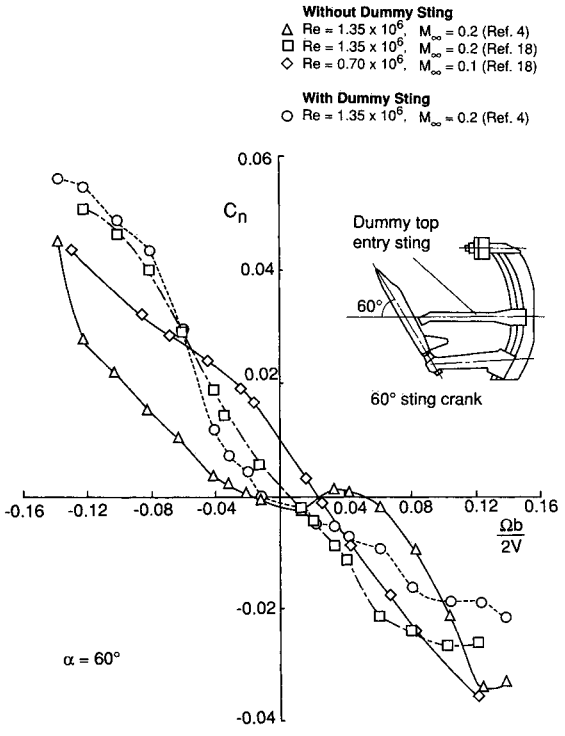


**Fig. 12 Yawing moment data for HIRM 2 in 4 × 2.7 m low-speed wind tunnel.**

When using a top-mounted dummy sting in addition to the aft sting support in the LSWT,[4] the dummy sting contributed appreciably to the total support interference at $\alpha = 40$ deg and $\alpha = 60$ deg, but not at $\alpha = 50$ deg. For the case of interest here $\alpha = 60$ deg, the support interference was confined to the yawing moment (Fig. 12). The results suggest that the interference was significant both with the aft sting alone and with the dorsal sting added.

*Analysis of the Rotary Data*

As will be shown, Reynolds number critical behavior in the presence of motion coupling and variable and/or fluctuating pressure gradients constitute a flow mechanism that is consistent with the observed behavior. In the absence of comprehensive aerodynamic data it is not possible to conclusively reconstruct the exact combination of factors that have contributed to the observed behavior. Nevertheless, it is instructive to speculate on the mechanisms that play a dominant role here. The interpretation of the rotary data is quite involved and only a brief account is given here; the complete analysis is the subject of a separate publication.[19]

The HIRM 2 fuselage is of a rounded rectangular cross section that transitions to a circular section forward of the canard[4] (see insert in Fig. 11). For the $Re = 1.35 \times 10^6$ condition the Reynolds number based on maximum fuselage width is approximately $0.40 \times 10^6$. Thus, the flow is subcritical for the rectangular section,[20] but subcritical/critical (transitional) on the circular section, $Re_d \leq 0.26 \times 10^6$.

The bistable trend at $\alpha = 60$ deg and $Re = 1.35 \times 10^6$ (Figs. 11 and 12) is likely the result of coupling between boundary-layer transition and the coning motion, or "moving wall effects" of the type described first by Ericsson and Reding.[20] The flow separation is apparently initially of the subcritical type[21] (i.e., dominated by laminar separation on the circular section) so that the translation of the forebody surface near the stagnation region delays flow separation on the advancing side and promotes it on the retreating side. The concomitant flow separation asymmetry generates a propelling side force until the critical coning rate is reached $\Omega b/2V \approx 0.03$, when transition occurs on the retreating side. This reverses the flow-separation/vortex asymmetry and a stable $C_n - \Omega b/2V$ trend develops with increasing rate. Because of the forebody geometry, the subcritical/critical interaction region is small and the effect on the vortex asymmetry, and therefore $C_n$, is gradual rather than abrupt as in the case of Malcolm's F-15 data.[3]

Because of the forebody shape transition, this interaction region is expected to be highly sensitive to small changes in the nonuniform pressure field. At $\alpha = 60$ deg the forebody vortex trails pass close to the rotor hub, where the lateral and radial deflections and burst positions are strong functions of position relative to the axis and of the parameters $\Omega b/2V$ and $V$. This determines the forebody flow characteristics and vortex shedding locations. Thus, it is quite plausible that a subtle change in test conditions such as a slight difference in the lateral alignment of the model or a small change in $V$ could have moved transition upstream in the separated layers, resulting in effectively critical flow separation characteristics.[21] In this case, coning motion will immediately move transition further upstream on the retreating side, delaying separation, and vice versa, on the opposite side.[22] This could have produced the stable $C_n - \Omega b/2V$ characteristic observed at $Re = 1.35 \times 10^6$ in the LSWT (Fig. 12). The tendency for this curve to level off at $\Omega b/2V \approx 0.06$ could be an indication of the reversal expected at higher rotation rates and accompanied by a smaller undamping side force.[22]

The effect of a change in freestream velocity can be seen in the $Re = 0.7 \times 10^6$ data (Fig. 12). The offset in this curve suggests that the resulting change in the interference flowfield has biased the vortex system to one side of the rotor arm, as was the case in Malcolm's data[3] at $\alpha = 70$ deg. Thus, the separation asymmetry is locked in by the support interference and the motion coupling becomes ineffective. A similar separation bias seems to have been produced at large negative coning rates by the dummy top-entry sting (Fig. 12), which is likely to have encouraged vortex shedding further forward on the forebody. It is interesting that the dummy does not completely disrupt the bistable behavior, reinforcing the notion that the rotor arm and hub are the primary source of interference at this angle of attack.

*Unsteady Wind-Tunnel Interference*

The observations in the large test section demonstrate a variety of types of nonlinear behavior consistent with this interpretation of the rotary aerodynamics of HIRM 2. In contrast, in the smaller facility the characteristics are nearly linear over the complete $\Omega b/2V$ range tested at both Reynolds numbers, with no hint of the $Re$-critical behavior expected at $Re = 1.35 \times 10^6$. This can be seen when the mirror images of the curves for negative rotation rates are superimposed on those for positive rates on the right side of Fig. 11 (Ref. 19). The fundamental difference between the nonlinearities observed in the two cases shows that quite different interference phenomena are at play in the two facilities.

The salient question is what interference mechanism could have produced the near-linear behavior at $Re = 1.35 \times 10^6$ in the TWT? The following explanation can be postulated. As the trailing tip vortices from the rotor arm sweep along the walls, the velocity deficient regions fluctuate longitudinally as described with reference to Fig. 10. The "dead" regions behind the rotor arm and around the hub expand due to the disturbances communicated from the walls. The forebody/canard leading-edge vortices are drawn laterally into the low-pressure regions. The regions of separated flow will expand with increasing rotation rate, while the low-pressure regions will shrink. Instead of simply spiraling outwards radially to form the helical structures, the vortex trails will be periodically deflected laterally. This oscillatory constraint on the radial motion of the vortex system, in concert with the effect of the oscillating pressure gradient on vortex shedding and breakdown, may be expected to inhibit the development of flow separation asymmetry on the forebody in a manner analogous to the effect of motion-induced unsteadiness on vortex shedding from an ogive-cylinder body[23] at $\alpha = 30$ deg.

The fluctuation of the separation asymmetry results in a zero time-averaged effect on $C_n$. Thus, the moving wall effects are overpowered, yielding to a type of unsteady vortex shedding normally found at higher angles of attack ($\alpha \geq 70$ deg).

Since the deflections and the intensity of the unsteady pressure gradients associated with the rotor interference all tend to increase with increasing rotation rate, the yawing moment would also increase with coning rate. Should this unsteady wind-tunnel interference become dominant, the resulting time-averaged $C_n - \Omega b/2V$ trend would be roughly linear as evidenced by the results at both Reynolds numbers in the smaller facility (Fig. 11). At high rates, the curves become slightly nonlinear as the vortex cores approach the limits of their displacement and the dependence on the pressure fluctuations near the rotor arm diminishes. The unsteady wind-tunnel interference is apparently negligible in the larger tunnel, allowing the existence of steady support interference.

Considering the Reynolds number effects observed (Figs. 11 and 12), dissimilar freestream turbulence levels in the two facilities could have had some influence; turbulence levels in the 2.4 × 1.8 m TWT are known to be higher than in the LSWT. Notwithstanding, the available data show that this could not account for the absence of appreciable nonlinearity in the trends obtained in the smaller wind tunnel. The $C_n - \Omega b/2V$ slope at low rates measured in the TWT at $Re = 1.35 \times 10^6$ is nearly identical to that for critical flow conditions in the LSWT, suggesting that the effects of dissimilar turbulence levels was not a factor. Moreover, an increase in turbulence level would move transition upstream in the separated layers. For turbulent separation an initially propelling side force would again be generated, albeit of smaller magnitude, with a reversal at some critical coning rate.[22] Therefore, the effect of an increase in turbulence would be to change the nonlinear behavior type but not to mask it. It is more likely that the nonlinearities associated with flow-separation/motion coupling have been eliminated by the unsteadiness generated by wind-tunnel interference.

While this explanation is not supported by conclusive data, it should be noted that the effects of various other parameters studied by O'Leary,[2,4] including angle of attack, are consistent with the present interpretation.[19] Nevertheless, it is clear that full confirmation of the hypothesis would require comprehensive flowfield measurements.

## Discussion

The two examples of unsteady wind-tunnel interference were analyzed in as much detail as the available data permit. While the precise interpretations of the observed phenomena are subject to further confirmation, there is no doubt as to the magnitude of the effects on unsteady as well as steady aerodynamic measurements for the aircraft configurations tested. The relative dimensions of the moving parts were similar in the two instances $b/w \approx b_s/w \approx 0.6$, and fairly typical of dynamic tests in high-speed wind tunnels. Clearly, methods are needed to quantify the interference effects or preferably, to eliminate them.

When one interference mechanism is dominant, the interference will be associated with a single convective time lag as was found for the SDM at high $\alpha$. In such cases, involving essentially pure unsteady wall interference, a quasisteady analysis combining static and dynamic data (such as that used to correct for support interference[8]) may be possible. On the other hand, for the more complex coupled interference mechanisms characterized by more than one time lag, the analytical approach is ruled out.[13] In many cases, as in the rotary experiment, the phenomena become even more complex due to coupling between the model motion and boundary-layer transition and/or flow separation.

While the low-$\alpha$ unsteady wind-tunnel interference encountered in the oscillatory tests probably cannot be eliminated in a ventilated test section housing a bulky test installation, experimental approaches are, in general, promising.

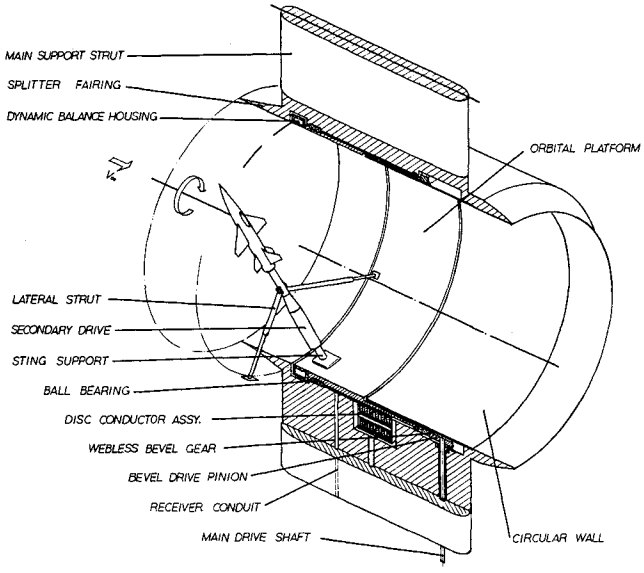


**Fig. 13 Layout of the OPLEC apparatus.**

It has been pointed out that the individual contributions of various sources of interference cannot be separated on a conventional rotary balance and a more sophisticated approach is required.[13] A rotary-balance technique offering the necessary flexibility was recently proposed.[13,14] The so-called orbital-platform, or OPLEC apparatus[15] illustrated in Fig. 13, makes it possible, in principle, to simulate separately—or in combination—the effects of the walls and of the rotating arm and fixed struts. Thus, the individual interference contributions can be determined in isolation or in the presence of coupling with the other flow mechanisms present.[13] Perhaps more significantly, application of the OPLEC concept could eliminate most of the problems identified here in connection with rotary balance testing; support interference is very low due to the absence of a centrally-mounted support arm and unsteady wall interference is negligible by virtue of the circular test section geometry (Fig. 13). For a detailed exposition of the concept see Ref. 15.

## Conclusions

An analysis of the limited oscillatory and rotary test results available for two aircraft configurations has revealed the existence of unsteady wind-tunnel interference phenomena involving coupling between support and wall interference mechanisms. While the interpretations given will require further confirmation, the postulated flow mechanisms are consistent with the observations. The following conclusions may be drawn.

1) Coupled support/wall interference can become severe under conditions typical of many dynamic tests in high-speed wind tunnels at both high and low $\alpha$.

2) Cross-coupling derivatives measured on the SDM at Mach 0.6 were significantly affected by unsteady wind-tunnel interference at low $\alpha$ ($\alpha = 10$ deg). At high $\alpha$ ($\alpha = 36$ deg) vortex-wake/wall interference was present instead.

3) The presence of significant unsteady wind-tunnel interference effects in a small test section precluded the measurement of the true Reynolds number critical yawing-moment characteristics of HIRM 2 at $\alpha = 60$ deg. In a larger wind tunnel these effects were absent and the prevalence of subcritical/critical fluid/motion coupling was determined by support interference effects.

4) Simple analytical corrections are not possible, but coupled interference could be assessed experimentally and effectively eliminated in the case of rotary balance testing by using the OPLEC concept. Unsteady interference in oscillatory experiments could be alleviated by testing in a solid-walled tunnel at a smaller test scale, i.e., with $b/w \leq 0.4$.

5) Identification of aircraft dynamic characteristics on the basis of dynamic wind-tunnel data at high $\alpha$ can be affected by the interpretation given to the prevailing interference phenomena.

## References


[1]Orlik-Rückemann, K. J., "Techniques for Dynamic Stability Testing in Wind Tunnels," Paper 1, AGARD-CP-235, Nov. 1978.

[2]"Rotary Balance Testing for Aircraft Dynamics," AGARD-AR-265, Dec. 1990.

[3]Malcolm, G. N., "Rotary-Balance Experiments on a Modern Fighter Aircraft Configuration at High Reynolds Numbers," AIAA Paper 85-1829, Aug. 1985.

[4]O'Leary, C. O., and Weir, B., "Effects of Reynolds Number, Mach Number and Sting Geometry on Rotary Balance Measurements," ICAS Paper 90-3.8.1, Sept. 1990.

[5]Beyers, M. E., "Subsonic Roll Oscillation Experiments on the Standard Dynamics Model," AIAA Paper 83-2134, Aug. 1983.

[6]Beyers M. E., "SDM Pitch- and Yaw-Axis Stability Derivatives," AIAA Paper 85-1827, Aug. 1985.

[7]Beyers, M. E., Szyszkowicz, M., and Cai, H. J., "Stability Derivatives of the Standard Dynamics Model at Mach 0.6," NRC, IAR-AN (to be published).

[8]Reding, J. P., and Ericsson, L. E., "Dynamic Support Interference," *Journal of Spacecraft and Rockets*, Vol. 9, No. 7, 1972, pp. 547–553.

[9]Beyers, M. E., "Some Recent Experiences of Support Interference in Dynamic Tests," NRC, NAE LTR-UA-83, Ottawa, Canada, Nov. 1985.

[10]Ericsson, L. E., and Reding, J. P., "Dynamic Support Interference in High-Alpha Testing," *Journal of Aircraft*, Vol. 23, No. 6, 1986, pp. 889–896.

[11]Ericsson, L. E., "Another Look at High-Alpha Support Interference," *Journal of Aircraft*, Vol. 28, No. 5, 1991, pp. 584–591.

[12]Beyers, M. E., "Wind-Tunnel Wall Interference in Rotary Balance Testing," NRC, NAE LTR-UA-90, Ottawa, Canada, Nov. 1987.

[13]Beyers, M. E., "Unsteady Wall Interference in Rotary Tests," AIAA Paper 89-0046, Jan. 1989.

[14]Beyers, M. E., "Wind Tunnel Wall Interference," *Rotary Balance Testing for Aircraft Dynamics*, AGARD AR-265, Dec. 1990, Chap. 5.2.

[15]Beyers, M. E., and Huang, X. Z., "The Orbital-Platform Concept for Nonplanar Dynamic Testing," NRC, NAE AN-52, Ottawa, Canada, May 1988.

[16]Laurmann, J. A., and Lukasiewicz, J., "Development of a Transonic Slotted Working Section in the NAE 30-Inch × 16-Inch Wind Tunnel," NRC, NAE LR-178, Ottawa, Canada, Aug. 1956.

[17]Coulter, S. M., and Marquart, E. J., "Cross and Cross-Coupling Derivative Measurements on the Standard Dynamics Model at AEDC," AIAA Paper 82-0596, March 1982.

[18]O'Leary, C. O., private communication, Oct. 1991.

[19]Beyers, M. E., "Analysis of Rotary Aerodynamics of Advanced Aircraft Configurations," NRC, IAR-LTR (to be published).

[20]Ericsson, L. E., and Reding, J. P., "Dynamics of Forebody Flow Separation and Associated Vortices," *Journal of Aircraft*, Vol. 22, No. 4, 1985, pp. 329–335.

[21]Chapman, D. R., Kuehn, D. M., and Larson, H. K., "Investigation of Separated Flows in Supersonic and Subsonic Streams with Emphasis on the Effect of Transition," NACA TN-3869, March 1957.

[22]Ericsson, L. E., and Reding, J. P., "Asymmetric Vortex Shedding from Bodies of Revolution," *Tactical Missile Aerodynamics*, Vol. 104, Progress in Astronautics and Aeronautics, AIAA, New York, 1986, pp. 243–296.

[23]Beyers, M. E., Huang, X. Z., Kapoor, K. B., and Peter, E., "Dynamic Stability Derivatives of a Secant-Ogive-Cylinder Configuration at High Angles of Attack," NRC, NAE-LTR-UA-89, Ottawa, Canada, Oct. 1987.